THE ADAPTIVE SPEED TRACKING CONTROLLER FOR INTELLIGENT ELECTRIC VEHICLES USING WFCMAC INCLUDES CAR-FOLLOWING BEHAVIOR, IMPROVING SAFETY AND ENERGY EFFICIENCY

BỘ ĐIỀU KHIỂN BÁM ĐUỔI TỐC ĐỘ THÍCH NGHI CHO XE ĐIỆN THÔNG MINH SỬ DỤNG WFCMAC CÓ TÍNH ĐẾN HÀNH VI BÁM THEO Ô TÔ, NÂNG CAO ĐỘ AN TOÀN VÀ HIỆU QUẢ NĂNG LƯỢNG

Tran Thanh Hai[1,*], Ngo Thanh Quyen[2], Nguyen Tho Van[2], Phan Minh Than[2], Nguyen Van Sy[3], Le Tong Tan Hoa[2], Bui Thi Cam Quynh[2]

DOI: http://doi.org/10.57001/huih5804.2024.289

ABSTRACT

Intelligent electric vehicles (IEVs) are increasingly being developed due to their high safety, energy-saving, and environmental friendliness. This research proposes an adaptive speed control method, especially considering the braking system of intelligent electric vehicles. The study aims to improve the safety and energy savings of IEVs during vehicle operation. First, the article builds a nonlinear dynamic model for IEVs, including electric motors, gearboxes, and braking systems. Then, an IEV acceleration controller will be designed using the Wavelet Function Cerebellar Model Articulation Controller (WFCMAC) to approximate the desired target. In addition, the paper also proposes a new regenerative braking strategy to maximize braking energy. Simulation results show that the proposed control system effectively keeps up speed and conserves braking energy while maintaining IEV's operational safety.

Keywords: *Intelligent electric vehicles; regenerative braking; energy efficiency; Wavelet Function Cerebellar Model Articulation Controller; adaptive control.*

TÓM TẮT

Các phương tiện xe điện thông minh (IEVs) ngày càng được phát triển do tính an toàn cao, tiết kiệm năng lượng và thân thiện với môi trường. Nghiên cứu này đề xuất phương pháp điều khiển thích nghi tốc độ, đặc biệt xét đến hệ thống phanh của xe điện thông minh. Nghiên cứu nhằm mục đích cải thiện sự an toàn và tiết kiệm năng lượng của IEVs trong quá trình vận hành xe. Đầu tiên, bài báo xây dựng mô hình động học phi tuyến cho IEVs, bao gồm động cơ điện, hộp số và hệ thống phanh. Sau đó, thiết kế một bộ điều khiển gia tốc IEV bằng phương pháp mạng điều khiển khớp nối mô hình tiểu não sử dụng hàm Wavelet (WFCMAC) để xấp xỉ mục tiêu mong muốn. Ngoài ra, bài báo còn đề xuất một chiến lược phanh tái tạo mới để tối đa hóa năng lượng phanh. Kết quả mô phỏng chỉ ra phương pháp đề xuất có hiệu quả tốt trong việc bám đuổi tốc độ và bảo toàn năng lượng phanh nhưng vẫn giữ tính an toàn vận hành của IEV.

Từ khoá: *Xe điện thông minh; phanh tái tạo; hiệu suất năng lượng; mạng điều khiển khớp nối mô hình tiểu não sử dụng hàm Wavelet; điều khiển thích nghi.*

[1]Office of Planning and Investment, Industrial University of Ho Chi Minh City, Vietnam

[2]Faculty of Electrical Engineering Technology, Industrial University of Ho Chi Minh City, Vietnam

[3]Faculty of Automotive Engineering Technology, Industrial University of Ho Chi Minh City, Vietnam

[*]Email: tranthanhhai@iuh.edu.vn

Received: 15/4/2024

Revised: 02/6/2024

Accepted: 27/9/2024

1. INTRODUCTION

Adaptive Cruise Control (ACC) adjusts vehicle speed based on traffic conditions [1, 2], aiming for safety and energy efficiency [3, 6]. However, balancing these objectives is challenging due to dynamic traffic. Machine learning algorithms like Model Predictive Control (MPC) have been explored to enhance ACC [7, 10] but face issues with unstable driving conditions. Consequently, there's a need for faster adaptive control systems for ACC. Frequent braking and acceleration in driving consume significant energy [11]. Regenerative Braking Systems (RBS) are crucial for improving energy efficiency, particularly with ACC. Optimizing energy recovery during braking is essential, with some studies suggesting using fuzzy logic for this purpose [12, 15].

This paper contributes to developing control systems for autonomous electric vehicles (IEVs) by creating a decentralized ACC system combined with RBS. The main contributions of this paper include:

1. Hierarchical ACC control system: The study has proposed a non-linear hierarchical control system, combining both the automatic cruise control system (ACC) and the regenerative braking system (RBS), which helps improve energy efficiency and ensure the safety of IEVs in various traffic situations.

2. CMAC model and Wavelet function: The study has applied a CMAC control model combined with Wavelet function to control IEVs and achieve desired states, providing a new and effective approach to controlling IEVs in autonomous vehicles.

The organization of this research paper unfolds as follows: Part 2 elucidates the nonlinear dynamic model of IEV. Part 3 delineates the hierarchical ACC control structure tailored for IEVs. Part 4 entails the execution of simulation experiments. Ultimately, Part 5 encapsulates the drawn conclusions.

2. THE NONLINEAR DYNAMIC MODEL OF IEV

Fig. 1 depicts the kinematics and control system of the IEV, including radar, AC induction motor (ACIM) active front axle control, power converter, speed transmission, and braking system on four wheels [16].

2.1. Vehicle Dynamics Model

Fig. 2 describes the vehicle dynamic model, which includes the front wheel's angular velocity (ω_f), the rear wheel's angular velocity (ω_r), and the actual speed in the vehicle's direction (v_h).

$$\begin{aligned} &m.\dot{v}_h=2.F_{xf}+2.F_{xr}-F_{res} \\ &J_{\varpi f}.\dot{\omega}_f=T_t-r.F_{xf}-T_{bf} \\ &J_{\varpi r}.\dot{\omega}_r=-r.F_{xr}-T_{br} \end{aligned} \quad (1)$$

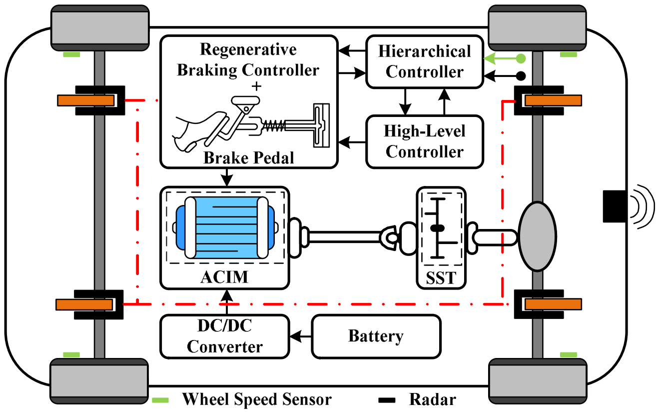

Fig. 1. Structural diagram of IEV

where, F_{xf} and F_{xr} represent the axial traction of the front and rear wheels, $J_{\varpi f}$ and $J_{\varpi r}$ are the rotational inertia, $T_t=T_m.\eta_g.i_g.i_0$ is the driving torque, η_g is the total efficiency of the gearbox and drive, i_g is the gear ratio of the gearbox, i_0 is the transmission ratio, r is the wheel radius, T_m is the torque from ACIM, $T_{bf}=\mu F_{\mu f}-T_{gen}$ and $T_{br}=\mu F_{\mu r}$ are the braking torques, $T_{gen}=\mu F_{\mu f}$ is the regenerative braking torque.

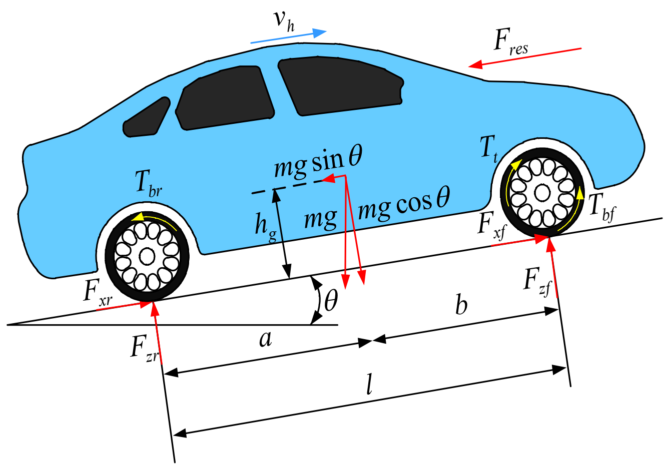

Fig. 2. Longitudinal dynamic model

F_{res} is the sum of various components of resistance forces that may occur in reality:

$$F_{res}=mg(f\cos\theta+\sin\theta)+0.5c_dA\rho v_h^2 \quad (2)$$

where, A is the vehicle frontal area, m is the vehicle's mass, f is the rolling friction coefficient, g is the gravitational acceleration, ρ is the air density, c_d is the aerodynamic resistance coefficient, and θ is the slope of the road.

2.2. Tired Dynamics Model

The force acts on the front F_{xf} and rear tires F_{xr} can be expressed as follows:

$$F_{xi}=D\sin\{C\arctan[B\lambda_i-E(B\lambda_i-\arctan(B\lambda_i))]\} \quad i=f, r \qquad (3)$$

λ_f and λ_r are the slip coefficients :

$$\lambda_i=(\omega_i r-v)/\max(\omega_i r,v) \qquad (4)$$

Tire longitudinal force coefficients B, C, D, E are defined as follows:

$$C=b_0;\ D=b_1F_{zi}^2+b_2F_{zi};\ B=\frac{b_3F_{zi}^2+b_4F_{zi}}{CDe^{b_5F_{zi}}};\quad E=b_6F_{zi}^2+b_7F_{zi}+b_8 \quad i=f, r \qquad (5)$$

F_{zf} and F_{zr} is the normal tire force :

$$F_{zf}=(gb-\dot{v}h_g)\frac{m}{2l};F_{zr}=(ga-\dot{v}h_g)\frac{m}{2l} \qquad (6)$$

where, l is the wheelbase, h_g is the height of the center of gravity, a and b are the distance from the center of gravity to the front and rear axles.

2.3. ACIM Dynamics Model

The torque response of ACIM approximates a first-order process [17]:

$$T_m=\frac{1}{\tau_m s+1}T_{des} \qquad (7)$$

3. DESIGN OF HIERARCHICAL CONTROLLER

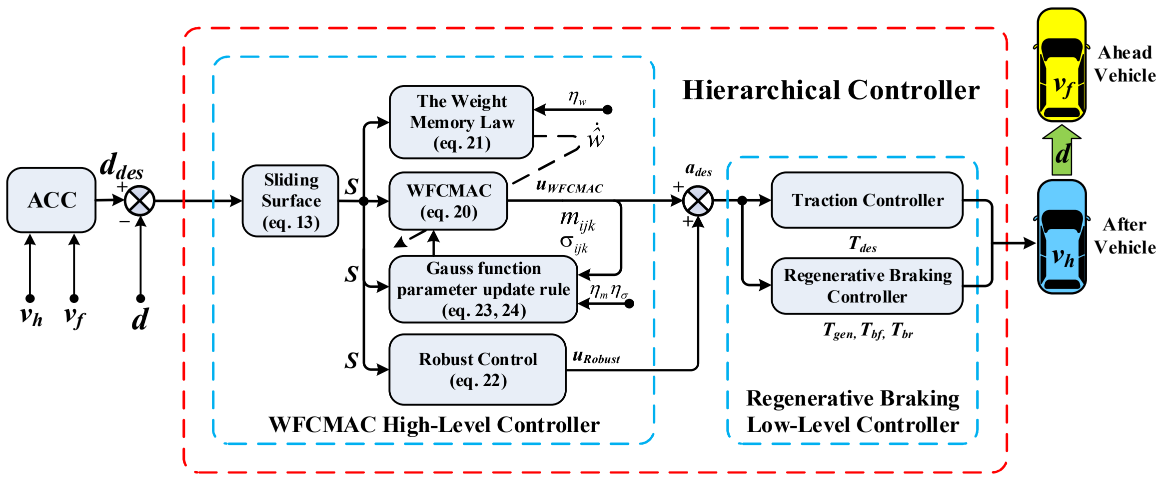

Fig. 3. ACC hierarchical control structure

The ACC model depicted in Fig. 3 is defined as follows:

$$\Delta\dot{d}=\Delta v-(\tau_1+\tau_2).a_h+\tau_2.a_f;\ \Delta\dot{v}=a_f-a_h;\ \dot{a}_h=\frac{K_L}{T_L}.a_{des}-\frac{1}{T_L}a_h \qquad (8)$$

where, $\Delta d = d - d_{safe}$ is the distance error, $\Delta v = v_f - v_h$ is the speed error, d is the actual distance, a_{des} is the desired acceleration, a_f is the actual acceleration of the ahead vehicle, a_h is the actual acceleration of the after vehicle. K_L and T_L is based on the empirical values of relevant vehicle models [18]. The safe distance between vehicles is based on the speed of the driving vehicle and a constant time gap:

$$d_{safe}=\tau_1.v_h+\tau_2.(v_h-v_f)+d_{min} \qquad (9)$$

where, d_{safe} is a safe distance, d_{min} is the minimum safe distance between vehicles, v_h is the speed of the after vehicle, v_f is the speed of the vehicle in front, τ_1 and τ_2 are positive constants found in [19]. The ACC model can be delineated as follows:

$$\begin{cases}\dot{x}=F_0(\underline{x})+G_0(\underline{x})u+L(\underline{x})\\ y=x\end{cases} \qquad (10)$$

where, $\underline{x}=[\Delta d,\Delta v,a_h]^T$, $u = a_{des}$, y is the system output, $L(\underline{x})$ is an uncertain component. For example, $F_0(\underline{x})$ and $G_0(\underline{x})$ are the identified nonlinear vector of the system and are used to model the system. Therefore, the nonlinear system (10) can be controlled and $G_0^{-1}(\underline{x})$ exists for all $\underline{x}$. The system tracking error is determined as follows:

$$e=y_d-y \qquad (11)$$

The system tracking error vector is defined as follows:

$$\underline{e}\triangleq\left[e^T\quad \dot{e}^T\quad \cdots\quad e^{(n-1)T}\right]^T \qquad (12)$$

The tracking error of the system is represented in vector form as follows:

$$s(\underline{e}(t))=e^{(n-1)}(t)+\zeta_1e^{(n-2)}(t)+\cdots+\zeta_{n-1}e(t)+\zeta_n\int_0^t e(t)dt \qquad (13)$$

where, $s=[s_1\ s_2\dots s_k]^T$ with i = 1, 2, 3,..., n. ζ_i is assumed to satisfy the Hurwitz polynomial.

If $F_0(\underline{x})$, $G_0(\underline{x})$ and $L(\underline{x})$ are precisely known, the ideal controller can be designed as follows:

$$u_{IDEAL} = G_0^{-1}(\underline{x})\left[\dot{x}_d - F_0(\underline{x}) - L(\underline{x}) + K^T \underline{e}\right]. \quad (14)$$

where, $K = [K_1^T \ \cdots \ K_n^T]^T$ is a positive constant matrix. However, $L(\underline{x})$ is indeterminate for practical applications. Therefore, u_{IDEAL} in (14) cannot be determined. This study proposes a control system consisting of a WFCMAC intelligent approximator and a robust controller:

$$u = u_{OPPROXIMATION} + u_{ROBUST} \quad (15)$$

where, $u_{OPPROXIMATION}$ is the main controller used to approximate the ideal controller; the robust controller u_{ROBUST} used to compensate for the approximation error between ideal controllers u_{IDEAL} and $u_{OPPROXIMATION}$.

3.1. WFCMAC High-Level Controller

3.1.1. Brief of the WFCMAC

The rules in the association layer of FCMAC are expressed as follows:

R^l if X_1 is μ_{1jk} and X_2 is $\mu_{2jk}, \cdots, X_{n_i}$ is μ_{ijk} then $O_{jk} = w_{jk}$

For $i = 1, 2, \ldots, n_i$, $j = 1, 2, \ldots, n_j$, $k = 1, 2, \ldots, n_k$, and $l = 1, 2, \ldots, n_k n_j$ (16)

where n_i is the number of the input dimension, n_j is the number of the layers for each input dimension, n_k is the number of blocks for each layer, $l = n_k n_j$ is the number of the fuzzy rules and μ_{ijk} is the fuzzy set for ith input, j^{th} layer and kth block, w_{jk} is the output weight in the consequent part. WFCMAC includes input, association memory, receptive field, and output spaces shown in Fig. 4.

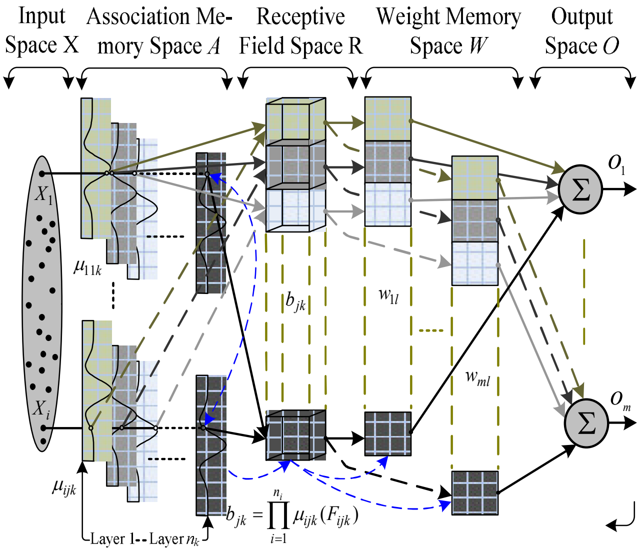

Fig. 4. WFCMAC controller structure

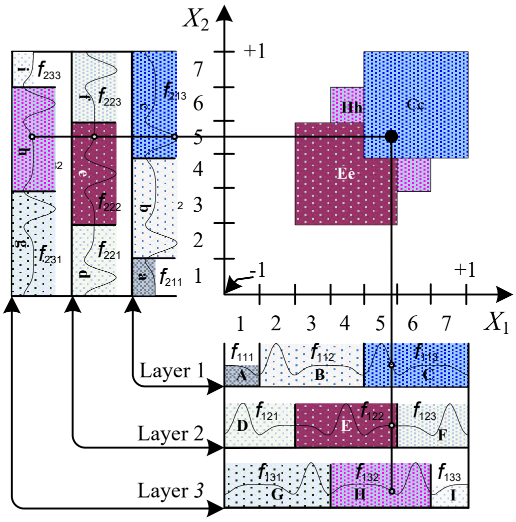

Fig 5. Block division of WFCMAC with wavelet function

a) The first mapping X: X → A: Each input state variable has the form $X = [X_1 \ X_2 \ \cdots \ X_{n_i}]$ and is defined as follows:

$$\mu_{ijk}(F_{ijk}) = -F_{ijk} \exp\left[-\frac{F_{ijk}^2}{2}\right], \quad (17)$$

where, $F_{ijk} = (X_i - m_{ijk})/\sigma_{ijk}$, σ_{ijk} is dilation, and m_{ijk} is translation.

b) The second mapping A: A → R: In the case of 2-D WFCMAC as depicted in Fig. 5, the content of the l^{th} hypercube can be acquired through the following method:

$$b_{jk} = \prod_{i=1}^{n_i} \mu_{ijk}(F_{ijk}) \quad (18)$$

c) Finally, the WFCMAC output is represented as follows:

$$u_{WFCMAC} = o = w^T b = \sum_{j=1}^{n_j} \sum_{k=1}^{n_k} w_{jk} b_{jk} \quad (19)$$

3.1.2. Adaptive WFCMAC control system

The update rule for the k^{th} weight memory is defined:

$$\dot{\hat{w}}_{jk} = -\beta_w \frac{\partial s\dot{s}}{\partial u_{WFCMAC}} \frac{\partial u_{WFCMAC}}{\partial \hat{w}_{jk}} = \beta_w s g(x) \hat{b}_{jk}(F_{ijk}) \quad (20)$$

$$\tau_{RC} = (2R^2)^{-1}[(I + H^2)R^2 + I]s^T(\underline{e}) \therefore \quad (21)$$

where, $R = \text{diag}[\xi_1, \xi_2]$ is the learning rate of the robust controller; β_w is the positive learning rate for the output weight memory w_{jk}. The dilations and translations of the k^{th} can also be updated according to

$$\dot{\hat{m}}_{ijk} = -\eta_m \frac{\partial s\dot{s}}{\partial u_{WFCMAC}} \frac{\partial u_{WFCMAC}}{\partial \hat{b}_{jk}} \frac{\partial b_{jk}}{\partial f_{ijk}} \frac{\partial f_{ijk}}{\partial \dot{\hat{m}}_{ijk}} = -\eta_m sg(x)\hat{w}_{jk} b_{jk} \frac{1-F_{ijk}^2}{(X_i - \hat{m}_{ijk})} \quad (22)$$

$$\dot{\hat{\sigma}}_{ijk} = -\eta_\sigma \frac{\partial s\dot{s}}{\partial u_{WFCMAC}} \frac{\partial u_{WFCMAC}}{\partial \hat{b}_{jk}} \frac{\partial b_{jk}}{\partial f_{ijk}} \frac{\partial f_{ijk}}{\partial \hat{\sigma}_{ijk}} = -\eta_\sigma sg(x)\hat{w}_{jk} b_{jk} \frac{1-F_{ijk}^2}{\hat{\sigma}_{ijk}} \quad (23)$$

where η_σ and η_m are positive learning rates for the dilation $\hat{\sigma}_{ijk}$ and translation $\hat{m}_{ijk}$.

3.2. Controller on the Lower Level for Regenerative Braking

3.2.1. Traction Controller: The desired tractive torque of an ACIM:

$$T_{des} = \frac{1}{i_g . i_0}(\dot{T}_{td} + \tau_m T_{td}) \quad (24)$$

where, $T_{td} = r(m.a_{des} + F_{res})$ is the desire traction torque of IEVs.

3.2.2. Strategy for Distributing Regenerative Braking

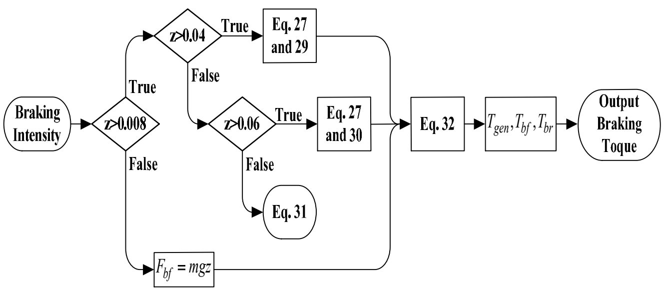

Fig. 6. Schematic of regenerative braking strategy

For optimal braking distance, braking force needs to meet the following criteria:

$$F_{bf} + F_{br} = mgz \quad (25)$$

Fig. 6 depicts the brake intensity flow chart. The detailed distribution of braking torque is provided as follows:

(1) 0 < z < 0.008: Throughout this scenario, for the optimization of braking energy reuse, the entirety of the necessary braking force is directed exclusively to the front wheels.

$$F_{br} = 0 \quad (26)$$

(1) 0. 008 < z < 0.04: During this case, the braking force is distributed as follows:

$$F_{br} = F_{bf} k_a \quad (27)$$

(2) 0.04 < z < 0.06: During this case, the braking force is distributed as follows:

$$F_{br} = F_{bf} k_b \quad (28)$$

(3) 0.06 < z < 1: This case is considered emergency braking to ensure vehicle safety [20]:

$$F_{bf,br\,max} = \mu F_{zf,zr} \quad (29)$$

Where, $F_{bf,br\,max}$ are the braking force for the largest front and rear wheels F_{bf} and F_{br}; k_a, k_b are the parameters; z is the braking intensity with $\frac{dv}{dt} = zg$; μ has a value of 0.5. Braking force is systematically applied to the brake mechanisms in a manner that mitigates the risk of wheel locking during braking maneuvers:

$$F_{\mu f} = \min(F_{bf}, \mu F_{zf}) \\ F_{\mu r} = \min(mgz - F_{\mu f}, \mu F_{zr}) \quad (30)$$

4. SIMULATION RESULTS

In this section, Matlab/Simulink is employed to simulate vehicle tracking control, validating the precision of the suggested control structure. An IEV model is constructed utilizing the parameters outlined in Table 1.

Table 1. Main parameters of the IEV model

Parameters	Value	Parameters	Value
m	1,346	i_0	3.5
ρ	1.206	θ	5.0
η_g	0.92	a	1.04
i_g	6.6732	b	1.04

The simulation depicts a vehicle moving on the road with a sequence of different fluctuations. Initially, it moves according to the journey of the vehicle in front, maintaining a speed of 12m/s. However, at time t = 200 seconds, the situation changes when the leading car decides to accelerate to 20m/s. A sudden brake occurred at time t = 400 seconds, causing the leading car to stop completely. This describes an incident that appears suddenly on the move. Besides, at time t = 800 seconds, the leading car begins to decelerate, creating a feeling of slowing down on the road. These situations often occur in traffic environments and require adaptation and quick processing by the controller.

Fig. 7 depicts the case of the control vehicle chasing the ahead vehicle in conditions where many events occur. When the ahead vehicle accelerates or decelerates, the control vehicle responds at speed (Fig. 7a) and maintains speed following the ahead vehicle (Fig. 7b). Depending on the speed of the ahead vehicle, the control vehicle will be able to automatically calculate to maintain the distance from the ahead vehicle (Fig. 7c) with distance error (Fig. 7d).

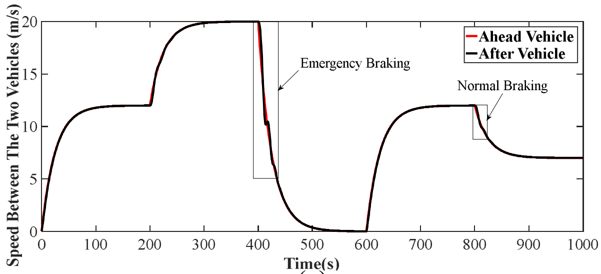

(a)

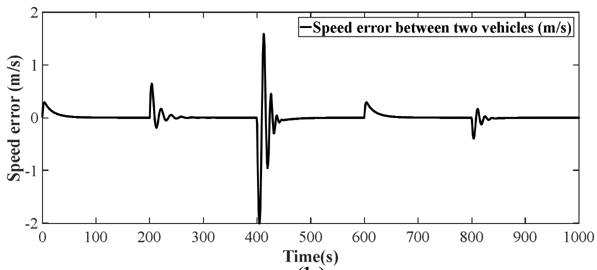

(b)

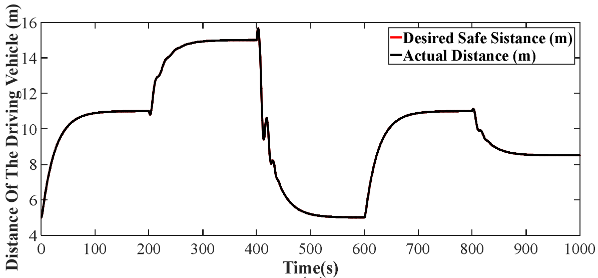

(c)

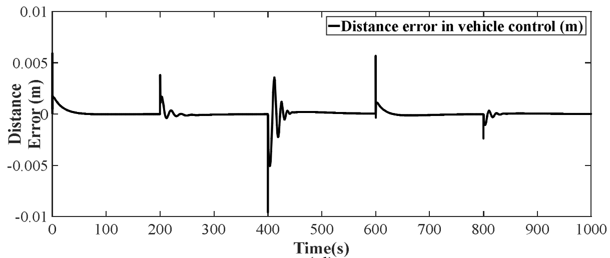

(d)

Fig. 7. Simulation results of chasing the ahead vehicle include: (a) Speed between the two vehicles; (b) Speed error between two vehicles; (c) Distance of the driving vehicle; (d) Distance error in vehicle control

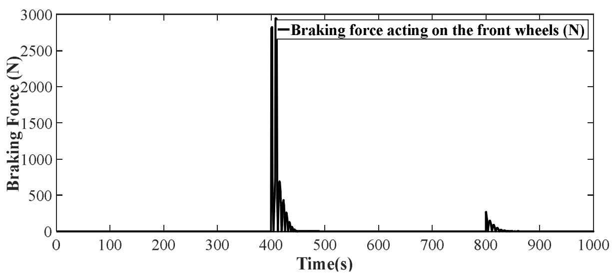

a)

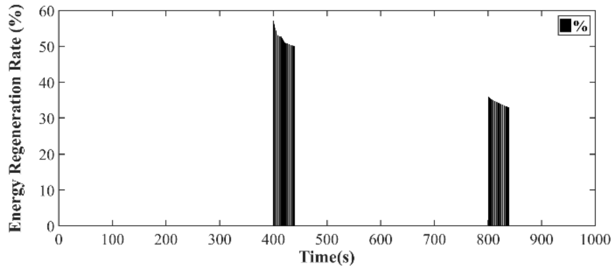

b)

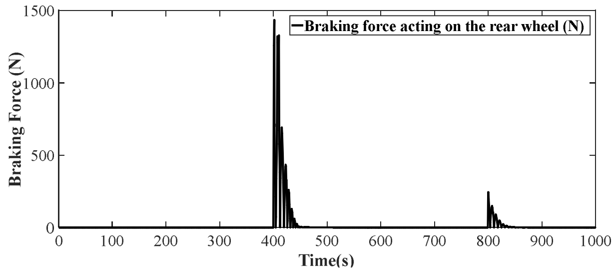

c)

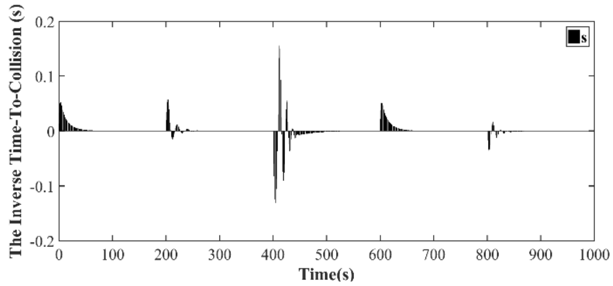

d)

Fig. 8. Results of parameters when the vehicle brakes suddenly and normally: (a) Braking force acting on the front wheels; (b) Braking force acting on the rear wheel; (c) Energy regeneration rate; (d) The inverse time-to-collision

Fig. 8 depicts the results when the vehicle brakes suddenly at t = 400 seconds and normal brakes at T = 800 seconds. During emergency braking, the braking force acting on the front wheel (Fig. 8a) is greater than the braking force acting on the rear wheel (Fig. 8b). However, when braking normally, the braking force will be distributed evenly across all wheels. When braking, the control vehicle has an energy regeneration rate (Fig. 8c) of about 50% (emergency braking) and about 35% (normal braking). The inverse collision time in Fig. 8d depicts that if the time is at a positive value, the vehicle is at a safe distance, and if it is at a negative value, then the vehicle has a high probability of collision [21].

5. CONCLUSION

This paper presents a hierarchical, non-linear ACC control system with renewable energy capabilities for electric vehicles. The proposed approach demonstrates robust stability in the face of disturbances caused by the ahead vehicle. Besides, the energy-saving performance of the new regenerative braking case is given an energy recovery rate of more than 50% for emergency braking and more than 35% for normal braking, respectively. In addition, this study provides essential information for designing an integrated controller of the ACC system and deploying it in applications that control vehicles following the ahead vehicle.

REFERENCES

[1]. L. Yu, R. Wang, "Researches on adaptive cruise control system: A state of the art review," *Proc. Inst. Mech. Eng. D* 236 (2–3), 211-240, 2022.

[2]. M. Althoff, S. Maierhofer, C. Pek, "Provably-correct and comfortable adaptive cruise control," *IEEE Trans. Intell. Veh*., 6 (1), 159-174, 2021.

[3]. B. Gao, K. Cai, T. Qu, Y. Hu, H. Chen, "Personalized adaptive cruise control based on online driving style recognition technology and model predictive control," *IEEE Trans. Veh. Technol*., 69 (11),12482-12496, 2020.

[4]. F. Lei, Y. Bai, W. Zhu, J. Liu, "A novel approach for electric powertrain optimization considering vehicle power performance, energy consumption and ride comfort," *Energy*, 167, 1040-1050,2019.

[5]. X. Lin, D. Görges, "Robust model predictive control of linear systems with predictable disturbance with application to multiobjective adaptive cruise control," *IEEE Trans. Control Syst. Technol*., 28 (4),1460–1475, 2020.

[6]. J. Chen, Y. Ye, Q. Wu, R. Langari, C. Tang, "Low-cost and high-performance adaptive cruise control based on inertial-triggered mechanism and multi-objective optimization," *IEEE Trans. Veh. Technol.*, 72 (6), 7279–7289, 2023.

[7]. X.W. Chen, J.G. Zhang, Y.J. Liu, et al., "Research on the intelligent control and simulation of automobile cruise system based on fuzzy system," *Math. Probl. Eng*., 2016.

[8]. J. Mao, L. Yang, Y. Hu, K. Liu, J. Du, "Research on vehicle adaptive cruise control method based on fuzzy model predictive control," *Machines*, 9 (8), 160, 2021.

[9]. Z. Cao, D. Yang, K. Jiang, T. Wang, X. Jiao, Z. Xiao, "End-to-end adaptive cruise control based on timing network," in *Proceedings of the 19th Asia Pacific Automotive Engineering Conference & SAE-China Congress*, Springer, 839–852, 2019.

[10]. B. Tian, G. Wang, Z. Xu, Y. Zhang, X. Zhao, "Communication delay compensation for string stability of CACC system using LSTM prediction," *Veh. Commun.*, 29, 100333, 2021.

[11]. G. Xu, K. Xu, C. Zheng, X. Zhang, T. Zahid, "Fully electrified regenerative braking control for deep energy recovery and maintaining safety of electric vehicles," *IEEE Trans. Veh. Technol.,* 65, 3, 1186–1198, 2016.

[12]. G. Xu, W. Li, K. Xu, Z. Song, "An intelligent regenerative braking strategy for electric vehicles," *Energies*, 4, 9, 1461–1477, 2011.

[13]. C. Qiu, G. Wang, M. Meng, Y. Shen, "A novel control strategy of regenerative braking system for electric vehicles under safety critical driving situations," *Energy*, 149, 329–340, 2018.

[14]. C. Jo, J. Ko, H. Yeo, T. Yeo, S. Hwang, H. Kim, "Cooperative regenerative braking control algorithm for an automatic-transmissionbased hybrid electric vehicle during a downshift," *Proc. Inst. Mech. Eng., D, J. Automobile Eng.,* 226, 4, 457–467, 2012.

[15]. L. Li, Y. Zhang, C. Yang, B. Yan, C. M. Martinez, "Model predictive control-based efficient energy recovery control strategy for regenerative braking system of hybrid electric bus," *Energy Convers. Manage.,* 111, 299–314, 2016.

[16]. J. Guo, W. Li, J. Wang, Y. Luo and K. Li, "Safe and Energy-Efficient Car-Following Control Strategy for Intelligent Electric Vehicles Considering Regenerative Braking," in *IEEE Transactions on Intelligent Transportation Systems*, vol. 23, no. 7, pp. 7070-7081, July 2022.

[17]. M. S. Basrah, E. Siampis, E. Velenis, D. Cao, S. Longo, "Wheel slip control with torque blending using linear and nonlinear model predictive control," *Vehicle Syst. Dyn.,* 55, 11, 1665–1685, 2017.

[18]. Wu D., Qiao B., Du C., Zhu Y., Yan F., Liu C., Li J., "Multi-objective dynamic coordinated Adaptive Cruise Control for intelligent electric vehicle with sensors fusion," *Mechanical Systems and Signal Processing*, 209, 111125, 2024.

[19]. X. Xia, Z. Meng, X. Han, H. Li, T. Tsukiji, R. Xu, Z. Zheng, J. Ma, "An automated driving systems data acquisition and analytics platform," *Transp. Res.*, 151, 104120, 2023.

[20]. L. Pugi, F. Grasso, M. Pratesi, M. Cipriani, A. Bartolomei, "Design and preliminary performance evaluation of a four wheeled vehicle with degraded adhesion conditions," *Int. J. Electr. Hybrid Vehicles,* 9, 1, 1–32, 2017.

[21]. Y. Zhang, M. Xu, Y. Qin, M. Dong, L. Gao, E. Hashemi, "MILE: Multiobjective Integrated Model Predictive Adaptive Cruise Control for Intelligent Vehicle," *IEEE Transactions on Industrial Informatics*, 19, 7, 8539-8548, 2023.

THÔNG TIN TÁC GIẢ

Trần Thanh Hải[1], Ngô Thanh Quyền[2], Nguyễn Văn Thọ[2], Phan Minh Thân[2], Nguyễn Văn Sỹ[3], Lê Tống Tân Hòa[2], Bùi Thị Cẩm Quỳnh[2]

[1]Phòng Kế hoạch - Đầu tư, Trường Đại học Công nghiệp thành phố Hồ Chí Minh

[2]Khoa Công nghệ Điện, Trường Đại học Công nghiệp thành phố Hồ Chí Minh

[3]Khoa Công nghệ Động lực, Trường Đại học Công nghiệp thành phố Hồ Chí Minh